# Selective Peptide Antagonist of the Class E Calcium Channel from the Venom of the Tarantula *Hysterocrates gigas*†

Robert Newcomb,*,‡ Balazs Szoke,‡ Andrew Palma,‡ Gang Wang,§ Xiao-hua Chen,‡ William Hopkins,‡ Ruth Cong,‡ Jim Miller,‡ Laszlo Urge,‡ Katalin Tarczy-Hornoch,‡ Joseph A. Loo,|| David J. Dooley,|| Laszlo Nadasdi,‡ Richard W. Tsien,⊥ José Lemos,§ and George Miljanich‡

*Elan Pharmaceuticals Inc., 3760 Haven Avenue, Menlo Park, California 94025, Department of Physiology, University of Massachusetts Medical Center, Worcester, Massachusetts 01655, Departments of Chemistry and Neuroscience Therapeutics, Parke-Davis Pharmaceutical Research Division of Warner Lambert Company, Ann Arbor, Michigan 48105, and Department of Molecular and Cellular Physiology, Beckman Center, Stanford University, Stanford, California 94305*

*Received May 27, 1998; Revised Manuscript Received August 11, 1998*

ABSTRACT: We describe the first potent and selective blocker of the class E $Ca^{2+}$channel. SNX-482, a novel 41 amino acid peptide present in the venom of the African tarantula, *Hysterocrates gigas*, was identified through its ability to inhibit human class E $Ca^{2+}$ channels stably expressed in a mammalian cell line. An $IC_{50}$ of 15−30 nM was obtained for block of the class E $Ca^{2+}$ channel, using either patch clamp electrophysiology or $K^+$-evoked $Ca^{2+}$ flux. At low nanomolar concentrations, SNX-482 also blocked a native resistant or R-type $Ca^{2+}$ current in rat neurohypophyseal nerve terminals, but concentrations of 200−500 nM had no effect on R-type $Ca^{2+}$ currents in several types of rat central neurons. The peptide has the sequence GVDKAGCRYMFGGCSVNDDCCPRLGCHSLFSYCAWDLTFSD-OH and is homologous to the spider peptides grammatoxin S1A and hanatoxin, both peptides with very different ion channel blocking selectivities. No effect of SNX-482 was observed on the following ion channel activities: $Na^+$ or $K^+$ currents in several cultured cell types (up to 500 nM); $K^+$ current through cloned potassium channels Kv1.1 and Kv1.4 expressed in *Xenopus* oocytes (up to 140 nM); $Ca^{2+}$ flux through L- and T-type $Ca^{2+}$ channels in an anterior pituitary cell line (GH3, up to 500 nM); and $Ba^{2+}$ current through class A $Ca^{2+}$ channels expressed in *Xenopus* oocytes (up to 280 nM). A weak effect was noted on $Ca^{2+}$ current through cloned and stably expressed class B $Ca^{2+}$ channels ($IC_{50}$ > 500 nM). The unique selectivity of SNX-482 suggests its usefulness in studying the diversity, function, and pharmacology of class E and/or R-type $Ca^{2+}$ channels.

The diversity of calcium channel isoforms and subtypes underlies a variety of roles for calcium in the regulation of neuronal function, including neurotransmission and neurosecretion, as well as cell membrane electrical activity and cellular metabolism (*1*, *2*). This diversity of structure and function makes brain calcium channels targets for the development of therapeutics (*3*): A peptide antagonist of the N-type calcium channel (SNX-111, or synthetic $\omega$-conopeptide MVIIA) is efficacious in animal models of chronic pain (*4*, *5*) and ischemic neuronal damage (*6*) and is currently in late stage clinical trials (*7*) for these applications in humans.

The mRNAs for the ion-conducting $\alpha$1 subunits of brain voltage-sensitive calcium channels have been categorized into five structural classes, A−E (*8*−*15*), while studies of native calcium channels have defined a variety of currents with distinctive electrophysiological and pharmacological properties (L, N, P, Q, R, and T; *16*−*20*, reviewed in refs *21* and *22*). Comparison of the properties of cloned and expressed channels and native currents suggests that class C and D mRNAs encode L-type currents (*8*, *23*−*25*), that class B mRNA encodes N-type currents (*26*, *27*), that class A mRNA encodes P- and Q-type currents (*13*, *28*, *29*).

Potent and selective antagonists are available for the L-, N-, and P/Q-type calcium channels, and these have provided valuable tools for the study of the function and pharmacology of these calcium channels. Organic compounds such as the dihydropyridines are antagonists of L-type calcium channels, while an increasing number of peptides from animal venoms provide antagonists of L-, N-, and P/Q-type calcium channels. Selective antagonists are used in in vitro experiments to elucidate the contribution of calcium channel subtypes to identified physiological processes and are used in whole animal experiments to define the pharmacological properties of antagonists of a particular subtype (see refs *3* and *30* for reviews).

The class E calcium channel is widely distributed in brain (*15*, *31*, *32*) and has been reported to possess electrophysiological and pharmacological properties most similar to native currents described as pharmacologically resistant or R-type. These properties include activation at higher transmembrane voltages (−30 to −10 mV), and resistance to block by agents that block N-, P/Q-, and L-type calcium currents (*19*, *31*, *33*−*35*). Furthermore, recent experiments

† J.L. and G.W. were supported by NIH Grant NS29740.
* Address correspondence to this author.
‡ Elan Pharmaceuticals Inc.
§ University of Massachusetts Medical Center.
|| Parke-Davis Pharmaceutical Research Division of Warner Lambert Co.
⊥ Stanford University.

10.1021/bi981255g CCC: $15.00 
Published on Web 10/16/1998

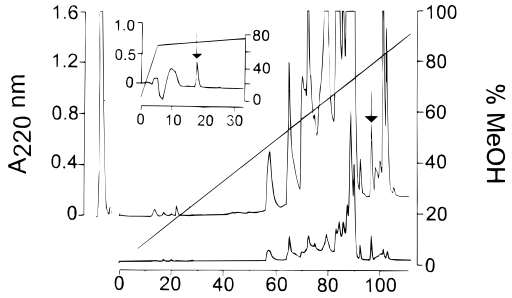


FIGURE 1: Isolation of SNX-482. Elution of 20 $\mu$L of the crude venom of *Hysterocrates gigas* by reverse-phase chromatography with 12 mM sodium phosphate, pH 6.2, as the aqueous buffer. The upper trace is the chromatogram obtained by monitoring absorbance, while the lower shows the UV fluorescence. The arrow indicates the elution of SNX-482. (Inset) Chromatogram of the resolution of SNX-482 by a third HPLC system using an aqueous buffer of 0.05% HFBA (after a second system using 0.1%TFA).

have shown that antisense oligonucleotides against the class E $\alpha$1 subunit reduce R-type currents in cerebellar granule cells (*36*). However, no selective high-affinity antagonist has yet been identified for the class E calcium channel. As a result, considerable uncertainty remains with regard to the diversity, function, and pharmacology of class E calcium channels.

As a step toward the further study and potential therapeutic modulation of the class E calcium channel, we describe here the isolation and characterization of a peptide, SNX-482, that is the first reported potent and selective antagonist of the class E calcium channel. We further describe the initial use of the peptide to survey the pharmacological properties of native R-type calcium currents.

## MATERIALS AND METHODS

*Purification*. The frozen liquid venom (20−150 $\mu$L) of adult male *Hysterocrates gigas* spiders (Invertebrate Biologics, Los Gatos, CA), was thawed, immediately injected onto a 4.5 × 250 mm wide-pore (octadecyl)silica HPLC[1] column (Vydac; particle size 5 $\mu$m), and eluted with a linear gradient of methanol in 12 mM sodium phosphate (pH 6.2) of 0−100% over 125 min at 1 mL/min. Elution was monitored by absorbance at 220 nm and by endogenous fluorescence (excitation 260 nm, emission 340 nm). Following localization of class E antagonist activity (see below and Figure 1), this peak was further fractionated with a gradient of 25−80% methanol in 0.1% TFA over 50 min. Edman degradation and amino acid analysis showed the material in the peak fraction to be 95−99% pure. The material from the TFA separation was rechromatographed with an aqueous buffer of 0.05% HFBA (65−85% over 50 min). The isolated peptide was of 99% or greater purity and was used to verify activity.

The spider peptide $\omega$-Aga-IIIA (*37*) was purified from the venom of *Agelenopsis aperta* (Spider Pharm, Feasterville, PA) for use as a positive control in several of the assays. Purification was over a Sephadex G-50 size-exclusion column, followed by two or three steps of reverse-phase HPLC (using the solvent systems described for SNX-482). Aga-IIIA provided by Dr. Mike Adams was used to monitor elution positions, and identity and concentrations were verified by amino acid analysis, Edman degradation, and mass spectral analysis.

*Amino Acid Analysis.* Amino acid analysis was performed by reverse-phase chromatography and fluorometric detection using the chiral analysis method involving derivatization of acid or enzymatic hydrolysates with *N*-acetyl-L-cysteine and OPA (*38*, *39*). Acid hydrolysis was with 6 M hydrochloric acid at 110 °C for 20 or 48 h with 50−70 pmol of peptide. Replicates of 3−8 analyses were used to calculate the amino acid composition of SNX-482, as well as to define concentrations used in the bioassays.

*Reduction and Alkylation.* SNX-482 (2 or 4 nmol of TFA-purified material) was derivatized with 4-vinylpyridine as described (*40*).

*Enzymatic Digestion.* Native or alkylated SNX-482 (250−500 pmol) was dried and digested with 0.3 $\mu$g of carboxypeptidase Y (Pierce) in 100 $\mu$L of 0.1 M sodium phosphate, pH 6.2. Aliquots of 10 $\mu$L were removed at various times, and OPA amino acid analysis was used to confirm the presence of a single tryptophan residue in SNX-482, as well as to confirm that the OPA-detectable amino acids were the L-enantiomers. The tryptophan determination was performed with native peptide, using long digests, since these did not proceed past the cystine residues. The analysis of amino acid chirality was performed with alkylated peptide, for which complete digestion of SNX-482 was obtained. Since the carboxypeptidase Y digest did not give clear sequence information at the carboxyl terminus of SNX-482, the carboxyl-terminal Ser-Asp sequence was obtained by digestion of native SNX-482 with agarose-bound carboxypeptidase A (Sigma), using the same digestion conditions as with the carboxypeptidase Y.

To confirm the results of Edman degradation, 1−2 nmol of native and alkylated SNX-482 was dried and digested with 1 $\mu$g of trypsin (Pierce or Worthington) in 50 $\mu$L of 0.1 M potassium phosphate, pH 7.4 (4 h at 37 °C). Fragments were resolved as above, using a gradient of 0−100% methanol in 0.1% TFA over 1 h and subjected to Edman degradation.

*Edman Degradation.* This was performed with an Applied Biosystems Model 120 Sequenator, using procedures recommended by the manufacturer.

*Mass Spectral Analysis.* Positive ion electrospray ionization−mass spectrometry analyses were performed with a Finnigan MAT 900Q forward geometry hybrid mass spectrometer. Mass spectra were acquired at full accelerating potential (5 kV) and a scan rate of 10 s decade$^{-1}$. The electrospray ionization interface used is based on a heated glass capillary inlet. Sample solutions were prepared in 80:15:5 (v/v/v) acetonitrile/water/acetic acid and infused through the ESI source at a flow rate of 1 $\mu$L min$^{-1}$. Matrix-assisted laser desorption/ionization mass spectra were acquired on a PerSeptive Vestec LaserTec Research time-of-flight mass spectrometer operating in the linear mode. Radiation from a nitrogen laser (337 nm) was used in the desorption process. Samples were prepared in a standard fashion by placing 1 $\mu$L of an aqueous solution of SNX-482 (1−10 pmol/$\mu$L in

[1] Abbreviations: BSA, bovine serum albumin; DMF, dimethylformamide; EDTA, ethylenediaminetetraacetic acid; EGTA, ethylene glycol bis($\beta$-aminoethyl ether)-*N*,*N*,*N*′,*N*′-tetraacetic acid; FMOC, fluorenylmethyloxycarbonyl; HEK, human embryonic kidney; HBTU, *O*-benzotriazole-*N*,*N*,*N*′,*N*′-tetramethyluronium hexafluorophosphate; HEPES, *N*-(2-hydroxyethyl)piperazine-*N*′-2-ethanesulfonic acid; HFBA, heptafluorobutyric acid; HPLC, high-performance liquid chromatography; MOPS, 3-(*N*-morpholino)propanesulfonic acid; OPA, *o*-phthaldialdehyde; TFA, trifluoroacetic acid.

0.1% TFA) and 1 $\mu$L of the appropriate matrix solution [approximately 5 mg/mL of either 3,5-dimethoxy-4-hydroxycinnamic acid or α-cyano-4-hydroxycinnamic acid in 1:2 (v/v) acetonitrile/0.1% TFA (aqueous)] on the sample target. The sample/matrix solution was then allowed to air-dry at room temperature prior to analysis.

*Synthesis of SNX-482.* The peptide was synthesized on a model 433A automated peptide synthesizer (Applied Biosystems) using standard FMOC chemistry. Fmoc-Asp (*tert*-butyl ester)-OH was coupled to chlorotrityl chloride functionalized resin. Standard HBTU/hydroxybenztriazole activation protocol and piperidine deprotection was used during the synthesis (*41*). The peptide was cleaved off the resin and deprotected in TFA/thioanisole/ethane dithiol/water (87.5/5/2.5/5 v/v/v/v) for 90 min. The crude linear peptide was subjected to air oxidation in a dilute buffered solution (potassium phosphate, pH 9.5) at 4 °C. The correctly folded product that coeluted with the native material was isolated by preparative HPLC with 15 mM ammonium acetate buffer and acetonitrile (*42*).

*Cell Lines.* The human neuroblastoma cell line IMR-32, the rat pituitary cell line GH-3, and the HEK cell line 293 were obtained from the American Type Culture Collection (Rockville, MD), and were grown as recommended. S3 and 192C cells are human embryonic kidney (HEK) cells that stably express the class B and class E calcium channels, respectively, and their preparation and use is described in ref *35*. In addition to the ion-conducting α1 subunits (human), both cell lines also express the auxiliary α2 and $\delta$ (human) and $\beta$1c (rabbit) calcium channel subunits. IMR-32 cells were differentiated by the addition of 1 mM dibutyryl-cAMP and 2.5 $\mu$M bromodeoxyuridine (both from Sigma) and were used 7−15 days after differentiation.

*INDO-1 Assay of Intracellular Calcium Increases.* Cells were detached with 0.5 mM EDTA, resuspended in 1% BSA-containing assay buffer (Hanks' solution without bicarbonate or phenol red containing 10 mM HEPES, brought to pH 7.5 with Tris base) at approximately $1 \times 10^7$cells/mL, and loaded with 5 $\mu$M INDO-1 acetoxymethyl ester (Molecular Probes, Eugene, OR) for 60 min at 30 °C. Test compounds or vehicle controls were incubated with approximately $5 \times 10^5$ loaded cells/mL in 0.5% BSA assay buffer for 10 min at 30 °C. Fluorescence measurements were made in triplicate with a Photon Technology International (South Brunswick, NJ) Model RF-F3004 spectrofluorometer thermostated at 30 °C. Excitation was at 350 nm and emissions were recorded at 400 and 490 nm. After acquiring emission signals for 20 s, cells were depolarized by the addition of a potassium chloride/calcium chloride stimulation solution to the stirred cuvette (final concentration 100 mM potassium, 8 mM calcium) and signals were acquired for an additional 30−50 s. The ratio of emissions (400 nm/490 nm) was plotted for initial evaluation. For dose−response curves, data were converted to intracellular calcium concentrations ($[Ca^{2+}]_i$) as described (*43*) and the difference between basal and peak (5−10 s after depolarization) emission values was calculated.

With IMR-32 cells, 5 $\mu$M nitrendipine, and for 192C cells, 15−45 $\mu$M valinomycin (to lower resting membrane potentials) was also included in the incubation mixture. For GH3 cells, peptide effects on peak calcium influx values were determined in the presence of 5 $\mu$M nitrendipine to estimate calcium flux through T-type channels, while the difference between basal and sustained (50 s after stimulation) emission ratios was measured without added nitrendipine to estimate flux through L-type channels. $IC_{50}$ values were obtained by fitting a four-parameter hyperbolic logistic function to the data by a weighted least-squares method. Experiments were repeated at least 3 times with each cell line, with each experiment involving 2−3 assays at each peptide concentration.

*Whole Cell Patch Clamp of Stably Transfected Cells.* Whole cell patch clamp (*44*) was performed with 2−6 MΩ electrodes with an Axopatch 200A amplifier interfaced to PCLAMP6 software (both Axon Instruments). Calcium currents were recorded with an external solution of the following (in millimolar): 100 tetraethylammonium chloride, 52 choline chloride, 15 sodium chloride, 2 calcium chloride, 0.8 magnesium chloride, 10 HEPES, and 7 glucose, with 0.1 mg/mL cytochrome *c*; adjusted to pH 7.4 with hydrochloric acid. The internal pipet solution consisted of the following (in millimolar): 140 cesium methanesulfonate**,** 5 EGTA, 10 HEPES, and 4 magnesium adenosine triphosphate; adjusted to pH 7.2 with cesium hydroxide. Peptide effects were assayed on currents elicited by changing the voltage from a holding potential of −90 to 0 mV, as a step pulse of 400 ms duration every 15 s. Data were sampled at 5 kHz and filtered at 1 kHz. Leak and capacitance currents were subtracted after measuring currents elicited by 22 mV hyperpolarizing pulses. Effects were quantitated on peak currents at steady state with peptide applied by flowthrough perfusion.

*Sodium and Potassium Currents in IMR-32 Cells.* These were recorded as previously described (*45*), but with an external bath of the following (in millimolar): 140 sodium chloride, 5 potassium chloride, 10 HEPES, 2 calcium chloride, 1 magnesium chloride, and 12 glucose, adjusted to pH 7.4 with sodium hydroxide. The internal pipet solution contained the following (in millimolar): 15 sodium chloride, 125 potassium methanesulfonate, 10 HEPES, 11 EGTA, 1 calcium chloride, 2 magnesium chloride, and 59 glucose, adjusted to pH 7.4 with potassium hydroxide. Cells were placed in a flowthrough chamber (0.5−1 mL/min) and SNX-482 was applied by flowthrough perfusion.

*Sodium and Potassium Currents in Retinal Ganglion Cells.* Retinal ganglion cells isolated from the retina of postnatal day 8 Sprague−Dawley rats express a mixture of 4-aminopyridine-sensitive and insensitive potassium conductances and a tetrodotoxin-sensitive sodium current. Retinal ganglion cells were prepared as described (*46*) using the immunopanning technique described in ref *47*. The extracellular solution for recording whole-cell potassium currents contained the following (in millimolar): 97 choline chloride, 2 potassium chloride, 0.8 magnesium chloride, 10 HEPES, pH 7.4, and 10 glucose. The intracellular solution for recording potassium currents contained the following (in millimolar): 88 potassium gluconate, 10 potassium chloride, 4 magnesium chloride, 10 MOPS, pH 7.25, 3 ATP, and 1 GTP. The extracellular solution for recording whole-cell sodium currents contained the following (in millimolar): 40 tetraethylammonium chloride, 59 sodium chloride, 0.8 magnesium chloride, 10 HEPES, pH 7.4, and 10 glucose. The intracellular solution for recording sodium currents contained the following (in millimolar): 98 cesium methane sulfonate, 4

magnesium chloride, 10 MOPS, pH 7.25, 3 ATP, and 1 GTP. Sodium and potassium currents were elicited by depolarizing voltage steps from a holding potential of −80 mV to a test potential of 0 mV for sodium currents and +30 mV for potassium currents. Peptides, 4-aminopyridine, and tetrodotoxin were dissolved in extracellular solution containing 0.1% BSA and were applied via the recording chamber superfusion system.

*Oocyte Assay: Class A Calcium Channel.* The cRNA for the class A α1 subunit (*13*) was expressed in *Xenopus* oocytes by standard methods (*48*). The cRNA for the α1 subunit was co-injected with cRNA for the rabbit α2 and δ (*49*) and human β (*10*) subunits in equimolar ratios. Approximately 50 nL was injected per oocyte, with a total cRNA concentration of 0.8 μg/μL. Currents were recorded by two-electrode voltage clamp in a solution containing the following (in millimolar): 4 barium chloride, 38 potassium chloride, 36 tetraethylammonium chloride, 5 4-aminopyridine, 0.4 niflumic acid, 5 HEPES (pH 7.5), and 0.1 mg/mL BSA. Data were sampled at 5 kHz and filtered at 1 kHz utilizing a OC-725B voltage-clamp amplifier (Warner Instruments) interfaced to PCLAMP software. Leak and capacitance currents were subtracted on-line by a P/4 protocol. Step pulses from −80 to 0 mV were used to elicit currents every 10 s. SNX-482 was applied by perfusion of the recording chamber.

*Oocyte Assay: Potassium Channels.* The cRNAs from the potassium channel α subunit cDNAs described in refs *50* (MKv1.1) and *51* (hKv1.2, hKv1.4) were injected into oocytes and the expressed potassium currents were analyzed 3−6 days later. The external recording solution contained the following (in millimolar): 115 sodium chloride, 2.5 potassium chloride, 1.8 calcium chloride, 10 HEPES pH 7.2, 0.1 mg/mL BSA. Other procedures were as with calcium channels, but test pulses were to +50 mV from a holding potential of −70 mV every 5 s.

*Neurohypophyseal Nerve Endings.* Nerve endings of the rat neurohypophysis were acutely dissociated and calcium currents recorded by the "perforated patch" technique as described (*52*). The cocktail of calcium antagonists used to isolate the resistant current included; nicardipine (2.5 μM), omega-conopeptides MVIIC (144 nM), and MVIIA (3 μM).

*Central Neurons.* Primary cultures of cerebellar granule cells were prepared as described (*19*) and hippocampal pyramidal cells were acutely dissociated as described (*53*). Primary cultures of retinal ganglion cells were obtained as described above. R-type currents were isolated by the protocol described (*19*). Cells were incubated for at least 30 min with 500 nM SNX-230 (synthetic ω-conopeptide MVIIC) in Tyrode solution (in millimolar: 119 sodium chloride, 5 potassium chloride, 2 calcium chloride, 1 magnesium chloride, 30 glucose, and 25 HEPES, pH 7.3) at room temperature. The R-type currents were recorded in 5 mM barium chloride (for hippocampal pyramidal and retinal ganglion cells) or 10 mM barium chloride (for granule cells) with 160 mM triethylamine chloride and 10 mM HEPES (pH 7.3) and 0.1 mg/mL cytochrome *c*. The internal solution contained the following (in millimolar): 108, cesium methanesulfonate, 4 magnesium chloride, 9 EGTA, 9 HEPES, 4 magnesium ATP, 14 creatine phosphate, and 0.3 GTP, pH 7.4). The series resistance was partially compensated (approximately 80%) and all currents were leak-subtracted by a hyperpolarizing P/4 procedure. A cocktail of calcium antagonists (10 μM nimodipine, 1−3 μM MVIIA, and 0.5 μM MVIIC) was used to isolate the resistant currents.

*Calcium Flux into Synaptosomes.* Rat neocortical synaptosomes were prepared and preincubated with peptides in 96 well plates for 5 min before addition of saline (*54*) with increased potassium (final concentration 30 mM) in combination with 1 μCi of calcium-45/mL (final volume 200 μL). Incubations were terminated by rapid filtration as described (*54*). The basal flux of calcium-45 was subtracted from the stimulated values, and percent effects were calculated relative to control values. Peptide effects were determined in triplicate in each experiment.

## RESULTS

### *Purification and Structure of SNX-482*

The venoms of 11 species of large terrestrial spiders were diluted to 0.5 μL of venom/mL, and whole cell patch clamp recording was used to determine inhibition of current flow through class E calcium channels stably expressed in human embryonic kidney (HEK) cells. Five venoms produced inhibition of calcium currents of greater than 50% without causing increases in leak current, and these were fractionated by HPLC on (octadecyl)silica at near neutral pH. The venom of *Hysterocrates gigas* reproducibly contained material that eluted between 70% and 80% methanol and antagonized the class E calcium current (arrow, Figure 1). This material was subjected to further analysis. Purification of >99%, as judged by Edman degradation and amino acid analysis, was achieved by two additional steps of reverse-phase chromatography at acidic pH in aqueous buffers of 0.1% TFA followed by 0.1% HFBA (inset, Figure 1). The class E calcium channel antagonist activity cochromatographed with the predominant material on both of these solvent systems. The purified material was denoted SNX-482. The yield of SNX-482 was typically 0.1−0.2 nmol/μL of venom.

Matrix-assisted laser desorption mass spectrometry gave an approximate molecular mass of 4500 for SNX-482, and endogenous fluorescence indicated the presence of tryptophan. On the basis of these results and the results of amino acid analysis, an amino acid composition was calculated that included 34 determined amino acids and assumed six cysteines and an undetermined number of proline residues; indicating SNX-482 to be a peptide of about 40−41 residues. Edman degradation of 0.5 nmol of the full-length Cys-alkylated peptide assigned the sequence up to position 35, showing the presence of six cysteine residues and a single proline residue. Trypsin was used to cleave 2 nmol of the alkylated peptide at position 23. Edman degradation of the carboxyl-terminal fragment gave the sequence of SNX-482 to position 39, while low yields of serine and aspartate (approximately 1 pmol) were obtained at positions 40 and 41. The amino-terminal portion of the sequence was verified by sequencing the remainder of the tryptic fragments. The carboxyl-terminal Ser-Asp sequence was verified by digestion with carboxypeptidase A, and both carboxypeptidases A and Y liberated the free carboxyl form of aspartate. Of those amino acids for which chirality was determined (i.e., all except proline, cysteine, and histidine), only the L-enantiomers were detected in acid and enzymatic hydroly-

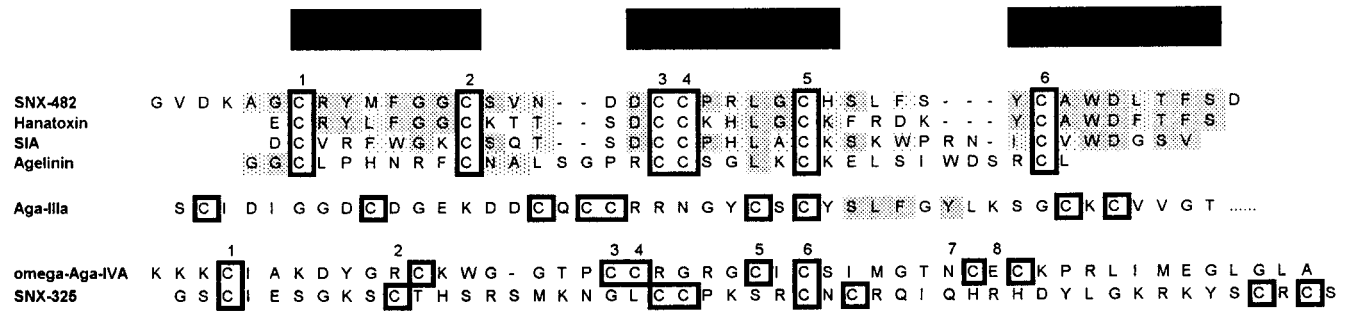


FIGURE 2: Structure of SNX-482 compared to structurally and functionally related polypeptides from spider venoms. The top part of the figure compares the structure of SNX-482 to that of other spider calcium and potassium antagonists with the same pattern of cysteine residues, including hanatoxin (*68*), $\omega$-grammatoxin S1A (*67*), and agelinin (*70*). The center part of the figure illustrates the amino-terminal sequence of the nonselective class E antagonist $\omega$-Aga-IIIA (*37*). The lower part of the figure illustrates the amino acid sequences of spider peptides that contain eight cysteine residues and that are selective for P/Q type ($\omega$-Aga IVA, *56*) or N-type (SNX-325, *45*) calcium channels.

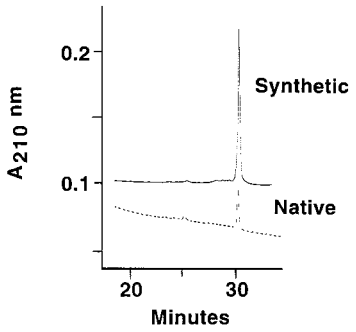


FIGURE 3: HPLC chromatograms of native and synthetic SNX-482. Elution conditions were as follows: solvent A, 20 mM potassium phosphate (pH 7.0); and solvent B, acetonitrile. Elution was with a linear gradient of 1% solvent B/min starting at 10% solvent B, at a flow rate of 1 mL/min over a Vydac (octadecyl)-silica column (300 Å pore size, 5 $\mu$M particle size, 4.6 × 250 mm).

sates. The sequence of SNX-482 is shown in Figure 2 and predicts a peptide of molecular mass 4495.07 Da. This was confirmed by electrospray mass spectrometry, which determined a molecular mass of 4495.00 Da.

To confirm the sequence and the assignment of biological activity, SNX-482 was chemically synthesized. The synthetic peptide had the identical retention time as the native peptide when chromatographed by reverse-phase HPLC (Figure 3).

*In Vitro Activity of SNX-482*

Material purified over two solvent systems was used to characterize the potency and selectivity of SNX-482. This material was typically 95−98% pure. In cases where bioactivity was observed, material purified over the third (HFBA) solvent system was used to verify the activity of SNX-482. This material was of ≥99% percent purity. The potency of SNX-482 against the stably expressed human class E calcium channel in the 192C cells was verified using both whole cell recording and depolarization-evoked changes in the fluoresence of the calcium indicator dye INDO-1. These results verified that both assay approaches provided, within error, equivalent dose−response data for SNX-482.

Both of the assay approaches, as well as a synaptosomal calcium flux assay, were used in a variety of assay systems to determine the selectivity of SNX-482 against calcium channel subtypes, as well as sodium and potassium channels.

These various assay systems used to examine the selectivity of SNX-482 against calcium channels are summarized in Table 1. Synthetic SNX-482 showed equal potency with the native material at blocking calcium flux through the class E calcium channels (assay with INDO-1 and the 192C cells).

Table 1: Calcium Channel Assay Systems

| subtype | preparation | subunits | species |
|---|---|---|---|
| | Cloned Channels | | |
| class E | HEK cells | α1E, $\beta$1c, α2-$\delta$ | human, human, rabbit |
| class B | HEK cells | α1B, $\beta$1c, α2-$\delta$ | human, human, rabbit |
| class A | oocyte | α1A, $\beta$1c, α2-$\delta$ | rabbit, human, rabbit |
| | Native Currents | | |
| N-type | IMR32 cells | native | human |
| L-type | GH3 cells | native | rat |
| T-type | GH3 cells | | |
| P/Q-type | cortical synaptosomes | native | rat |
| R-type | posterior pituitary | native | rat |
| | granule cells | native | mouse |
| | retinal ganglion cells | native | mouse |
| | hippocampal pyramidal cells | native | mouse |

*Effects of SNX-482 on Class E Calcium Currents.* Whole cell patch clamp electrophysiology was performed on HEK cells stably expressing class E calcium channels (*35*). A typical trace of the recorded calcium current in the presence and absence of 33 nM SNX-482 is illustrated in Figure 4A, and the time course of effect is illustrated in Figure 4B. The dose−response relationship is summarized in Figure 4C. The $IC_{50}$ for block of the class E current by SNX-482 is approximately 30 nM. Figure 4C also summarizes effects of Aga-IIIA on the class E current ($IC_{50}$ 3−10 nM).

Initial experiments assessing the effects of SNX-482 on depolarization-evoked calcium flux used HEK cells stably expressing the class E channel. Representative time courses for the potassium-evoked increase in the INDO-1 fluorescence ratio (400/490 nm), in the presence and absence of SNX-482, are illustrated in the inset of Figure 5A. SNX-482 produced a potent block of the INDO-1 signal change in these cells. The dose−response of the effect on the peak change in fluorescence is plotted in Figure 5A, as is a comparison to the effects of Aga-IIIA. An $IC_{50}$ of between 10 and 30 nM was consistently obtained for the SNX-482 effect in a number of experiments. The depolarization evoked increase in internal calcium in these cells was resistant to MVIIC (1 $\mu$M), MVIIA (1 $\mu$M), and nitrendipine (5 $\mu$M) (not illustrated). Thus, the results with the calcium-sensitive dye essentially duplicate the results obtained by electrophysiology with the same cells.

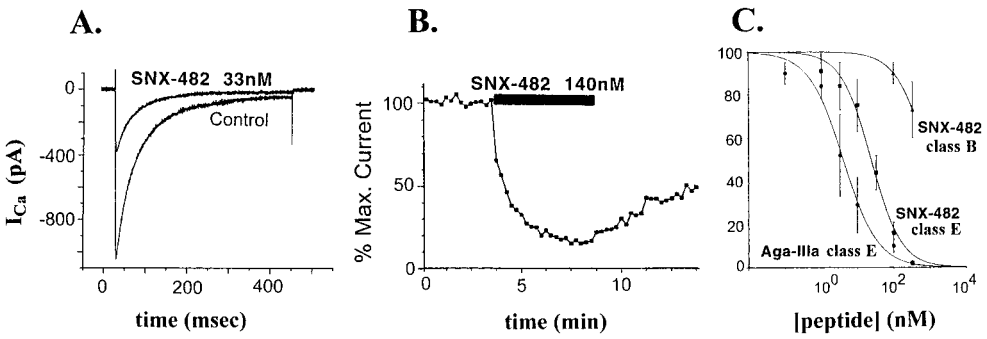


FIGURE 4: Antagonism of the class E calcium current by SNX-482. (A) Waveform of the calcium current measured in 192C cells in the presence and absence of 33 nM SNX-482 by whole cell patch clamp. The current is elicited by a pulse to 0 mV from a holding potential of −90 mV. (B) Peak amplitude over time of the calcium current elicited in 192C cells as in panel A, with perfusion of 140 nM SNX-482 as indicated. (C) Dose−response relationship of the peak inward calcium current in HEK cells stably expressing class E (192C cells) and class B α1 subunits in the presence of varying concentrations of SNX-482. For comparison purposes, the effects of Aga-IIIA on the class E current are also illustrated. The data were obtained as illustrated in panels A and B. Each data point is the mean and standard deviation from 3−5 independent measurements at each concentration, with one cell being used at one or two concentrations.

*Selectivity of SNX-482: Lack of Effects against Other Ion Channels*

*Class B and N-type Calcium Currents.* Effects of SNX-482 on the cloned expressed class B calcium channel were determined by patch clamp electrophysiology using HEK cells stably expressing the cloned class B calcium channel (*35*). Data were obtained as described for the class E currents, and Figure 4C summarizes the resulting concentration−effect data. SNX-482 has slight effects on the class B calcium channel but the $IC_{50}$ is well over 500 nM.

The IMR-32 neuroblastoma cell line contains a significant amount of calcium current that possesses the hallmarks of the N-type calcium channels: sensitivity to ω-conopeptide GVIA and intermediate activation and inactivation kinetics (*55*). Effects of SNX-482 on the native N-type calcium channel were evaluated with these cells, using the fluorescent calcium indicator dye INDO-1 to measure calcium flux. Flux through the N-type channel was evaluated in the presence of 5 μM nitrendipine, which was added to block the contribution of the L-type current in these cells. Consistent with the presence of a significant amount of N-type current in these cells, SNX-194 (the methionine-12 → norleucine-12 derivative of ω-conopeptide MVIIA) nearly completely inhibited the remaining transient depolarization-dependent increase in internal calcium with an apparent $IC_{50}$ of 1 nM (Figure 5C). SNX-482 had an effect on calcium flux through the N-type channel only at relatively high concentrations (30−50% block at 300−500 nM, Figure 5C), confirming the results obtained by patch clamp recording of the stably expressed class B current.

*Class A and P/Q-type Calcium Currents.* The *Xenopus* oocyte expression system was used to investigate the effects of SNX-482 on the barium current through the class A calcium channel. At 250 nM SNX-482 and 4 mM barium, no effect of the peptide was observed (inhibition <5−10%, three independent experiments, data not illustrated). Preliminary data (Xiao-hua Chen, unpublished results) suggest that the dose−response effects of SNX-482 on the class E current are similar in 4 mM barium and 2 mM calcium.

As an independent method of checking the activity of SNX-482 on the class A calcium channel, effects on calcium fluxes into cortical synaptosomes were assayed. This assay is sensitive to blockers of the class A or P/Q-type calcium channel, and consistent with previous results (*54*), the influx of calcium-45 into neocortical synaptosomes was, in four independent experiments, always blocked between 40% and 50% by two different antagonists of the class A calcium channel: MVIIC at 300 nM (*30*) and Aga-IVA at 300 nM (*56*). In the same experiments, 300 nM SNX-482 always blocked less than 10% of the evoked calcium flux (data not illustrated). These results independently confirm the data obtained with oocytes showing a lack of effect of SNX-482 on the class A or P/Q-type calcium channel.

*L-type Calcium Currents.* The anterior pituitary cell line, GH3, is reported to exhibit both L- and T-type calcium currents by whole cell patch clamp recording of barium currents (*57*). Consistent with this, the dihydropyridine nitrendipine blocked only a sustained component (no inactivation over 69 s) of the depolarization-evoked increase in internal calcium, as monitored by changes in the fluorescence ratio (400 nm/490 nm) of the calcium-sensitive dye INDO-1 (inset, Figure 5B) The apparent $IC_{50}$ for this inhibition was approximately 400 nM.

SNX-482, at concentrations of 500−600 nM, had no effect (<10%) on the total internal calcium increase in GH3 cells evaluated at 40 s after depolarization and thus did not affect the L-type component of the signal. As a positive control, we showed that Aga-IIIA produced a potent but partial block of the depolarization evoked signal (apparent $IC_{50}$ 1.5 nM, evaluated at 60 s after depolarization), consistent with its reported potent block of the L-type current in myocytes (*58*). Concentration−effect data for the peptides and dihydropyridines are summarized in Figure 5B.

*T-type Calcium Currents.* The transient increase in internal calcium remaining after nitrendipine block of the INDO-1 signal in GH3 cells was completely blocked by felodipine (apparent $IC_{50}$ 600 nM, Figure 5B). This dihydropyridine completely blocks the T-type calcium channel in myocardial cells at concentrations of 4 μM (*58*). These data provide strong pharmacological evidence that depolarization-evoked calcium flux into GH3 cells has contributions from both L- and T-type calcium channels. SNX-482, at 600 nM, had no effect on the peak internal calcium (at 10 s after depolarization) in the presence of 5 μM nitrendipine, indicating lack of activity against the T-type calcium channel ($n = 3$ independent experiments).

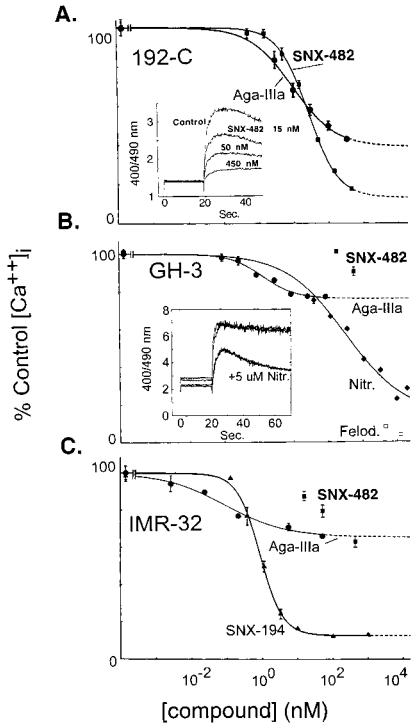


FIGURE 5: Effects of SNX-482 on depolarization-evoked changes in INDO-1 fluorescence. The effects of SNX-482 on depolarization evoked increases in internal calcium are compared to those of $\omega$-Aga-IIIA and positive controls. The data are the means and standard deviations of triplicate determinations for representative assays, which were each repeated 3−4 times with similar results. (A) Effects of SNX-482 and Aga-IIIA on the evoked increases in internal calcium in the 192C (class E expressing) cells. The inset shows the time course in the change of the fluorescence ratio (400 nm/490 nm) with different concentrations of SNX-482 included in the assay. (B) Dose-dependent effects of SNX-482, Aga-IIIA, and the dihydropyridines nitrendipine (Nitr.) and felodipine (Felod.) on sustained increase in internal calcium in GH3 cells. The data illustrated were evaluated at 50 s, and reflect more the L-type (nitrendipine-sensitive) signal. The inset shows the time course of the depolarization-evoked increase in the fluorescence ratio (400 nm/490 nm) and illustrates that addition of 5 $\mu$M nitrendipine only partially blocks total signal. The more rapidly decaying component observed in the presence of nitrendipine is blocked by felodipine but is unaffected by 500 nM SNX-482. (C) Effects of SNX-482, Aga-IIIA, and SNX-194 (the methionine to norleucine analogue of SNX-111, which is synthetic $\omega$-conopeptide MVIIA) on the peak in internal calcium after potassium depolarization of IMR-32 cells.

*Sodium and Potassium Currents.* At 250 nM, SNX-482 had no effect on the potassium current in IMR-32 neuroblastoma cells (less than 4% variation in peak current, $n$ = 3). At 500 nM, SNX-482 had no effect on either sodium or potassium currents in retinal ganglion cells maintained in primary culture (less than 4% effect on peak current, $n$ = 3). At 140 nM, SNX-482 had no effect on the cloned potassium channels Kv1.1 ($n$ = 2), and Kv1.4 ($n$ = 2) expressed in *Xenopus* oocytes.

### *Effects of SNX-482 on Native Resistant Calcium Currents*

The above studies defined SNX-482 as a potent and selective antagonist of the class E type calcium channel. Since considerable uncertainty remains as to the native currents that correspond to the class E calcium channel, SNX-482 was tested on a variety of currents that share an important pharmacological property of the class E calcium channel: that is, resistance to selective blockers of N-, P/Q-, and L-type

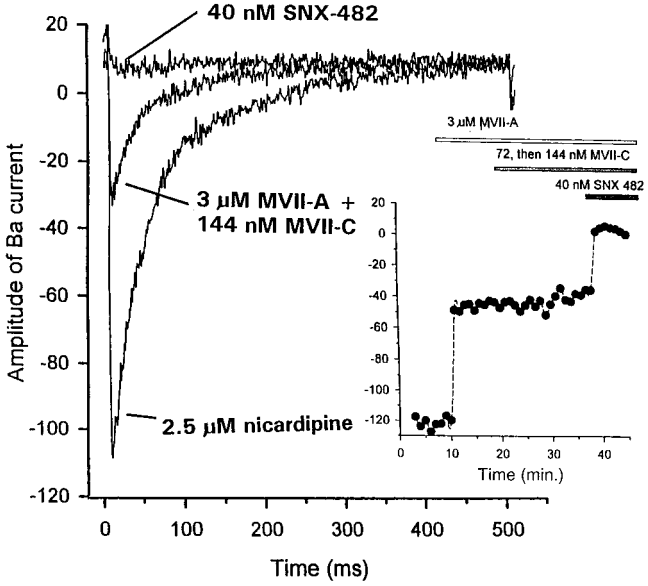


FIGURE 6: Effects of SNX-482 on a resistant calcium current in posterior pituitary nerve endings. Whole terminal barium current was recorded from the isolated nerve terminals of the rat neurohypophysis using the perforated patch technique. Macroscopic barium currents (in 5 mM $Ba^{2+}$) were elicited by depolarizations from −80 to +10 mV. The largest currents illustrated in the traces at left were recorded after block of L-type currents with 2.5 $\mu$M nicardipine. The N-type calcium channel blocker SNX-111 (synthetic $\omega$-conopeptide MVIIA, 30) was added at 3 $\mu$M and blocked a large part, but not all, of the transient current illustrated. Subsequent perfusion of the P/Q-type channel blocker SNX-230 (synthetic MVIIC, *30*) at 72 and then 144 nM had no effect on the remaining current in the terminal illustrated. Perfusion of SNX-482 at 40 nM blocked the current that was resistant to the above calcium blockers. The inset shows the time course of the amplitude of the peak current at a time resolution of 1 min/point, with the bars indicating application of each compound.

currents (see Materials and Methods section for composition of the cocktail of blockers used). Neuronal cell body preparations included cerebellar granule cells ($n$ = 3) (*19*), retinal ganglion cells ($n$ = 2) (*59*), and hippocampal pyramidal cells ($n$ = 3) (*60*). In addition, we studied effects of SNX-482 on the recently described R-type current in acutely dissociated neurohyphophyseal nerve endings (*52*).

SNX-482 caused potent block of one of these four R-type currents. When applied to the neurohypophyseal nerve endings at 40 nM, SNX-482 produced near-complete block of this current (Figure 6). In replicate experiments, 40 nM SNX-482 blocked 91% of the resistant current (±12% SEM, $n$ = 4) and 4 nM blocked 48% (±10%, $n$ = 3). By contrast to the posterior pituitary nerve endings, the R-type currents obtained with the neuronal cell body preparations were insensitive to SNX-482 (data not illustrated). In the presence of 200−500 nM SNX-482, the R-type currents in neuronal cell bodies were reproducibly 90−98% that recorded in the absence of the peptide. The magnitude of these R-type currents typically varied from 50 to 250 pA. Even at concentrations of 1 $\mu$M, SNX-482 had no significant effect on R-type calcium currents in the retinal ganglion cells and hippocampal pyramidal cells.

## DISCUSSION

A number of polypeptide calcium channel antagonists have been isolated from the venoms of cone snails and spiders

(*30*), with a few peptide antagonists isolated from the mamba snake venoms (*61*, *62*). The calcium antagonists from mamba venoms are structurally distinct from spider and cone snail calcium antagonists and are structurally unrelated to SNX-482. The cysteine pattern of SNX-482 (C−C−CC−C−C) is the same as that of the $\omega$- and $\delta$-peptides from cone snail venoms, which are, respectively, ligands for voltage-sensitive calcium and sodium channels (*30*, *63*−*66*). The $\delta$-conopeptides are somewhat similar to SNX-482 in that both are acidic and have a significant number of hydrophobic residues, while the $\omega$-conopeptides are highly basic and tend to otherwise consist primarily of small or polar amino acids. Other than in the pattern of cysteine residues, there are no obvious sequence homologies between known cone snail peptides and SNX-482. Among known peptides with the C−C−CC−C−C cysteine framework, SNX-482 is unique in having significant extensions of amino acid sequence at both ends of the cysteine residues.

The primary sequence of SNX-482 is related to several peptides that contain the C−C−CC−C−C framework of cysteine residues and that have been isolated from spider venoms. These include grammatoxin S1A (*67*), and hanatoxin (*68*), which have been isolated from the venom of the tarantula *Grammostola spatulata.* Sequence comparisons for this group of peptides are shown at the top part of Figure 2. S1A is a blocker of both N- and P/Q-type, but not L-type, calcium channel subtypes (*67*, *69*), and hanatoxin is a potassium channel antagonist (*68*) whose activity on other cation channels has not yet been reported. Although the degree of homology is less, there is also structural similarity with the calcium antagonist agelinin from *Agelina opulenta* (*70*). There is no apparent homology in the non-cysteine amino acids with calcium antagonists from spider venoms that contain greater than six cysteine residues, some examples of which are shown in the lower part of Figure 2.

Among those peptides that are homologous to SNX-482, a distinct pattern of amino acid substitutions is observed in the comparison with hanatoxin. The amino acid sequences of the two peptides are nearly identical in the regions between the first and second cysteine residues and between the fourth and fifth cysteine residues, as well as in the carboxyl-terminal extension following the sixth cysteine residue. By contrast, the sequences between the second and third cysteine residues as well as between the fifth and sixth cysteine residues are divergent.

Our studies of in vitro activity show that SNX-482 is a selective and potent blocker of the class E calcium channel. Although the peptide does have a slight effect on the N-type (class B) calcium channel, the potency of block of the N-type channel is substantially less than that observed with the class E channel and the posterior pituitary R-type current. This degree of selectivity compares favorably with other peptide calcium antagonists. For example, the N-channel-selective peptides SNX-325 and $\omega$-conopeptide GVIA are similar to SNX-482 in that they block one type of calcium channel at low nanomolar concentrations but block additional calcium channels at micromolar concentrations (*45*, *71*). Other peptide calcium antagonists such as MVIIC, S1A, and Aga-IIIA have lower degrees of selectivity than does SNX-482.

In the studies reported here, we have used a variety of assay systems to determine selectivity of SNX-482. Technically, lack of effect in some assay systems could be due to minor differences across assay systems, such as differences in composition of auxiliary subunits, or species differences in the ion-conducting $\alpha$1 subunits. However, experiments in progress ($n = 3$) show that SNX-482 at $\geq$200 nM has no detectable effect on the total voltage-activated barium current of the cerebellar granule cells used in the assay of isolated R-type currents described above. Since cerebellar granule cells contain significant components of N-, L-, and P/Q-type current (*19*), lack of block of total barium current by SNX-482 independently confirms lack of block of N-, L-, and P/Q-type currents.

In the absence of selective pharmacological antagonists of the class E subtype of calcium channel, considerable uncertainty has remained with regard to the structural identity and diversity of calcium currents that are high-voltage-activated but also pharmacologically resistant to blockers of N-, P/Q-, and L-type currents (*19*, *72*−*75*). We have shown that SNX-482 potently blocks the R-type calcium current through a cloned and expressed human $\alpha$1E subunit, as well as through a native R-type current in rat neurosecretory nerve endings. Both these currents are, unlike the low-voltage-activated T-type calcium current, activated at higher transmembrane voltages. The simplest explanation of these results is that the R-type current observed in the posterior nerve endings reflects the activity of a class E calcium channel.

By contrast, SNX-482 has no effect on pharmacologically resistant calcium currents in several rat central neuron preparations, including the cultured cerebellar granule cells originally used to describe the R-type current (*19*). Since the concentration of SNX-482 required for effective block of the neurohypophyseal R-type current has no effect on N-, L-, and P/Q-type currents, the current blocked in the pituitary nerve endings is pharmacologically distinct from R-type pituitary currents that we tested in neuronal cell bodies.

In conclusion, on the basis of the results presented here, we believe that SNX-482, as well as its synthetic and naturally occurring analogues, will be a useful tool for further defining both calcium channel diversity and the potential therapeutic benefits of a new class of novel selective calcium channel antagonists.

## ACKNOWLEDGMENT

We thank our colleagues at Neurex and Parke-Davis who participated in the early stages of this work, including Dr. David Rock for his initial observations of the effects of SNX-482 on cerebellar granule cells, as well as members of the Neurex synthetic chemistry group. We thank Dr. Mike Adams for providing Aga-IIIA and Dr. Adams and Dr. Brian Whiteley for advice on spider peptides and venoms. We thank Joann Geer, Ege Kavalali, and Karl Deisseroth for technical assistance.

## REFERENCES

1. Dunlap, K., Luebke, J. I., and Turner, T. J. (1995) *Trends Neurosci. 18*, 89−98.
2. Tsien, R. W., and Wheeler, D. B. (1998) Voltage gated calcium channels, in *Intracellular Calcium* (Carafoli, E., and Klee, C. B., Eds.) Oxford University Press, New York.
3. Miljanich, G. P., and Ramachandran, J. (1995) *Annu. Rev. Pharmacol. Toxicol. 35*, 707−734.

4. Malmberg, A. B., and Yaksh, T. L. (1994) *J. Neurosci. 14*, 4882−4890.
5. Bowersox, S. S., Gadbois, T., Singh, T., Pettus, M., Wang, Y., and Luther, R. R. (1996) *J. Pharmacol. Exp. Ther. 279*, 1243−1249.
6. Valentino, K. V., Newcomb, R., Gadbois, T., Singh, T., Bowersox, S., Bitner, S., Justice, A., Yamashiro, D., Hoffman, B. B., Ciaranello, R., Miljanich, G., and Ramachandran, J. (1993) *Proc. Natl. Acad. Sci. U.S.A. 90*, 7894−7897.
7. McGuire, D., Bowersox, S., Fellman, J. D., and Luther, R. R. (1997) *J. Cardiovasc. Pharmacol. 30*, 400−403.
8. Mikami, A., Imoto, K., Tanabe, T., Niidome, T., Mori, Y., Takeshima, H., Narumiya, S., and Numa, S. (1989) *Nature 340*, 230−233.
9. Williams, M. E., Brust, D. H., Feldman, D. H., Patthi, S., Simerson, S., Maroufi, A., McCue, A. F., Velicelebi, G., Ellis, S. B., and Harpold, M. M. (1992a) *Science 257*, 389−395.
10. Williams, M. E., Feldman, D. H., McCue, A. F., Brenner, R., Velicelebi, G., Ellis, S. B., and Harpold, M. M. (1992b) *Neuron 8*, 71−84**.**
11. Snutch, T. P., Leonard, J. P., Gilbert, M. M., Lester, H. A., and Davidson, N. (1990) *Proc. Natl. Acad. Sci. U.S.A. 87*, 3391−3395.
12. Starr, T. V., Prystay, W., and Snutch, T. P. (1991) *Proc. Natl. Acad. Sci. U.S.A. 88*, 5621−5625.
13. Mori, Y., Friedrich, T., Kim, M. S., Mikami, A., Nakai, J., Ruth, P., Bosse, E., Hofmann, F., Flockerzi, V., Furuichi, T., Mikoshiba, K., Imoto, K., Tanabe, T., and Numa, S. (1991) *Nature 350*, 398−402.
14. Seino, S., Chen, L., Seino, M., Blondel, O., Takeda, J., Johnson, J. H., and Bell, G. I. (1992) *Proc. Natl. Acad. Sci. U.S.A. 89*, 584−588.
15. Soong, T. W., Stea, A., Hodson, C. D., Dubel, S. J., Vincent, S. R., and Snutch, T. P. (1993) *Science 260*, 1133−1136.
16. Carbone, E., and Lux, H. D. (1984) *Nature 310*, 501−502.
17. Nowycky, M. C., Fox, A. P., and Tsien R. W. (1985) *Nature 316*, 440−443.
18. Llinas, R., Sugimori, M., Hillman, D. E., and Cherksey, B. (1992) *Trends Neurosci. 15*, 351−354.
19. Randall, A., and Tsien, R. W. (1995) *J. Neurosci. 15*, 2995−3012.
20. Zhang, J. F., Ellinor P. T., Aldrich, R. W., and Tsien, R. W. (1993) *Neuropharmacology 32*, 1075−1088.
21. Tsien, R. W., Ellinor, P. T., and Horne, W. A. (1991) *Trends Neurosci. 12*, 349−354.
22. Randall, A., and Tsien, R. W. (1998) In *Low Voltage Activated T-type Calcium Channels* (Tsien, R. W., Clozel, J.-P., and Nargeot, J., Eds.) pp 29−43, Adis Press, Basel, Switzerland.
23. Biel, M., Ruth, P., Bosse, E., Hullin, R., Stuhmer, W., Flockerzi, V., and Hofmann, F. (1990) *FEBS Lett. 269*, 409−412.
24. Perez-Reyes, E., Kim, H. S., Lacerda, A. E., Horne, W., Wei, X., Rampe, D., Campbell, K. P., Brown, A. M., and Birnbaumer, L. (1989) *Nature 340*, 233−236.
25. Tanabe, T., Takeshima, H., Mikami, A., Flockerzi, V., Takashi, H., Kangawa, K., Kojima, M., Matsuo, H., Hirose, T., and Numa, S. (1987) *Nature 328*, 313−318.
26. Dubel, S. J., Starr, T. V. B., Hell, J., Ahlijanian, M. K., Enyeart, J. J., Catterall, W. A., and Snutch, T. P. (1992) *Proc. Natl. Acad. Sci. U.S.A. 89*, 5058−5062.
27. Fujita. Y., Mynlieff, M., Dirkson, R. T., Kim, M. S., Niidome, T., Nakai, J., Friedrich, T., Iwabe, N., Miyata, T., Furuichi, T., Furutama, D., Mikoshiba, K., Mori, Y., and Beam, K. G. (1993) *Neuron 10*, 585−598.
28. Sather, W. A., Tanabe, T., Zhang, J. F., Mori, Y., Adams, M. E., and Tsien, R. W. (1993) *Neuron 11*, 291−303.
29. Stea, A., Tomlinson, W. J., Soong, T. W., Bourinet, E., Dubel, S. J., Vincent, S. R., and Snutch, T. P. (1994) *Proc. Natl. Acad. Sci. U.S.A. 91*, 10576−10580.
30. Olivera, B. M., Miljanich, G. P., Ramachandran, J., and Adams, M. E. (1994) *Annu. Rev. Biochem. 63*, 823−867.
31. Williams, M. E., Marubio, L. M., Deal, C. R., Hans, M., Brust, P. F., Philipson, L. H., Miller, R. J., Johnson, E. C., Harpold, M. M., and Ellis, S. B. (1994) *J. Biol. Chem. 269*, 22347−22357.
32. Yokoyama, C. T., Westenbroek, R. E., Hell, J. W., Soong, T. W., Snutch, T. P., and Catterall, W. A. (1995) *J. Neurosci. 10*, 6419−6432.
33. Forti, L., Tottene, A., Moretti, A., and Pietrobon, D. (1994) *J. Neurosci. 14*, 5243−5256.
34. Bezprozvanny, I., and Tsien, R. W. (1995) *Mol. Pharmacol. 48*, 540−549.
35. Rock, D. M., Horne, W. A., Hashimoto, C., Zhou, M., Palma, D., Hidayetoglu, D., and Offord, J. (1998) In *Low Voltage Activated T-type Calcium Channels* (Tsien, R. W., Clozel, J.-P., and Nargeot, J., Eds.) pp 279−289, Adis Press, Basel, Switzerland.
36. Piedras-Renteria, E. S., and Tsien R. W. (1998) *Proc. Natl. Acad. Sci. U.S.A. 95*, 7760−7765.
37. Venema, V. J., Swiderek, K. M., Lee, T. D., Hathaway, G. M., and Adams, M. E. (1992) *J. Biol. Chem. 267*, 2610−2615.
38. Bruckner, H., Wittner, R., and Godel, H. (1989) *J. Chromatogr. 476*, 73−82.
39. Newcomb, R., Sun, X., Taylor, L., Curthoys, N., and Giffard, R. (1997) *J. Biol. Chem. 272*, 11276−11282.
40. Hawke, D., and Yuan, P. (1987) *Appl. Biosystems User Bull. 28*, 1-8.
41. Fields, G. B., and Noble, R. L. (1990) *Int. J. Pept. Protein Res. 35*, 161−214.
42. Urge, L., Szoke, B., Newcomb, R., Miljanich, G., Chung, D., Hom, D., Silva, D., Tran-Trau, P., and Nadasdi, L. (1997) *Soc. Neurosci. Abstr.* 472.2.
43. Grynkiewicz, G., Poenie, M., and Tsien, R. (1985) *J. Biol. Chem. 260*, 3440−3450.
44. Hamill, O. P., Marty, A., Neher, E., Sakmann, B., and Sigworth, F. J. (1981) *Pflugers Arch. 391*, 85−100.
45. Newcomb, R., Palma, A., Fox, J., Gaur, S., Lau, K., Chung, D., Cong, R., Bell, J. R., Horne, B., Nadasdi, L., and Ramachandran, J. (1995) *Biochemistry 34*, 8341−8347.
46. Meyer-Franke, A., Kaplan, M. R., Pfrieger, F. W., and Barres, B. A. (1995) *Neuron 15*, 805−819.
47. Barres, B. A., Silverstein, B. E., Corey, D. P., and Chun, L. L. (1988) *Neuron 1*, 791−803.
48. Hopkins, W. F., Demas, V., and Tempel, B. L. (1994) *J. Neurosci. 14*, 1385−1393.
49. Ellis, S. B., Williams, M. E., Ways, N. R., Brenner, R., Sharp, A. H., Leung, A. T., Campbell, K. P., McKenna, E., Koch, W. J., Hui, A., Schwartz, A., and Harpold, M. M. (1988) *Science 241*, 1661−1664.
50. Tempel, B. L., Jan, Y. N., and Jan, L. Y. (1988) *Nature 332*, 837−839.
51. Ramaswami, M., Gauta, M., Kamb, A., Rudy, B., Tanouye, M. A., and Mathew, M. K. (1990) *Mol. Cell. Neurosci. 1*, 214−223.
52. Wang, G., Dayanithi, G., Kim, S., Hom, D., Nadasdi, L., Kristipati, R., Ramachandran, J., Stuenkel, E. L., Nordmann, J. J., Newcomb, R., and Lemos, J. (1997) *J. Physiol. 502* (2), 351−363.
53. Kavalali, E. T., Zhuo, M., Bito, H., and Tsien, R. W. (1997) *Neuron 18*, 1−20.
54. Geer, J. J., Dooley, D. J., and Adams, M. J. (1993) *Neurosci Lett. 158*, 97−100.
55. Carbone, E., Sher, E., and Clementi, F. (1990) *Pflugers Arch. 416*, 170−179.
56. Mintz, I. M., Venema, V. J., Swiderek, K. M., Lee, T. D., Bean, B. P., and Adams, M. E. (1992) *Nature 355*, 827−9.
57. Lievano, A., Bolden, A., and Horn, R. (1994) *Am. J. Physiol. 267 (Cell Physiol.)*, C411−C424.
58. Cohen, C. J., Ertel, E. A., Smith, M. M., Venema, V. J., Adams, M. E., and Leibowitz, M. D. (1994) *Mol. Pharmacol. 42*, 947−951.
59. Taschenberger, H., and Grantyn, R. (1995) *J. Neurosci. 15*, 2240−2254.
60. Mintz, I. M., Adams, M. E., and Bean, B. P. (1992) *Neuron 9*, 85−95.

61. De Weille, J. R., Schweitz, H., Maes, P., Tartar, A., and Lazdunski, M. (1991) *Proc. Natl. Acad. Sci. 88*, 2437−2440.
62. Schweitz, H., Heurteaux, C., Bois, P., Moinier, D., Romey, G., and Lazdunski, M. (1994) *Proc. Natl. Acad. Sci. 91*, 878−882.
63. Olivera, B. M., Rivier, J., Scott, J. K., Hillyard, D. R., and Cruz, L. J. (1991) *J. Biol. Chem. 266*, 22067−22070.
64. Woodward, S. R., Cruz, L. J., Olivera, B. M., and Hillyard, D. R. (1990) *EMBO J. 9*, 1015−1020.
65. Hasson, A., Fainzilber, M., Gordon, D., Zlotkin, E., and Spira, M. E. (1993) *Eur. J. Neurosci. 5*, 56−64.
66. Shon, K. J., Hasson, A., Spira, M. E., Cruz, L. J., Gray, W. R., and Olivera, B. M. (1994) *Biochemistry 33*, 11420−11425.
67. Lampe, R. A., Defeo, P. A., Davison, M. D., Young, J., Herman, J. L., Spreen, R. C., Horn, M. B., Mangano, T. J., and Keith, R. A. (1993) *Mol. Pharmacol. 44*, 451−460.
68. Swartz, K. J., and MacKinnon, R. (1995) *Neuron 15*, 941−949.
69. Piser, T. M., Lampe, R. A., Keith, R. A., and Thayer, S. A. (1995) *Mol. Pharmacol. 48*, 131−139.
70. Hagiwara, K., Sakai, T., Miwa, A., Kawai, N., and Nakajima, T. (1990) *Biomed. Res. 11*, 181−186.
71. Wang, X. M., Treistman, S. N., and Lemos, J. (1992) *J. Physiol. 445*, 181−199.
72. Bourinet, E., Zamponi, G. W., Stea, A., Soong, T. W., Lewis, B. A., Jones, L. P., Yue, D. T., and Snutch, T. P. (1996) *J. Neurosci. 16*, 4983−4993.
73. Marubio, L. M., Rosenfeld, M., Dasgupta, S., Miller, R. J., and Philipson, L. H. (1996) *Receptors Channels 4*, 243−251.
74. Tottene, A., Moretti, A., and Pietrobon, D. (1996) *J. Neurosci. 16*, 6353−6363.
75. Stephans, G. J., Page, K. M., Burley, J. R., Berrow, N. S., and Dolphin, A. (1997) *Pflugers Arch.—Eur. J. Physiol. 433*, 523−532.

BI981255G